



1 **The response of diazotrophs to nutrient amendment in the**
2 **South China Sea and western North Pacific**

3

4 Zuozhu Wen^{1,2}, Thomas J. Browning², Rongbo Dai¹, Wenwei Wu¹, Weiyang Li^{1,a},

5 Xiaohua Hu¹, Wenfang Lin¹, Lifang Wang¹, Xin Liu¹, Zhimian Cao¹, Haizheng Hong¹,

6 and Dalin Shi¹

7

8 ¹State Key Laboratory of Marine Environmental Science, Xiamen University, Xiamen,

9 Fujian, PR China

10 ²Marine Biogeochemistry Division, GEOMAR Helmholtz Centre for Ocean Research

11 Kiel, Germany

12

13 *Correspondence to:* Dalin Shi (dshi@xmu.edu.cn) and Haizheng Hong

14 (honghz@xmu.edu.cn)

15

16 a. Present address: Key Laboratory of Marine Ecosystem Dynamics, Second Institute of

17 Oceanography, Ministry of Natural Resources, Hangzhou, Zhejiang, PR China



18 **Abstract.** The availability of iron (Fe) and phosphorus (P) have been shown to be key
19 factors regulating rates of nitrogen fixation in the western Subtropical Pacific. However,
20 their relative importance at finer spatial scales between the northern South China Sea
21 (NSCS) and the western boundary of the North Pacific is poorly constrained.
22 Furthermore, nutrient limitation of specific diazotroph types has not yet been assessed.
23 Here we investigated these unknowns by carrying out measurements of (i) finer scale
24 spatial variabilities in N₂ fixation rates and diazotroph abundances throughout these
25 regions, and (ii) conducting eight additional Fe and phosphate addition bioassay
26 experiments where both changes in N₂ fixation rates and the abundances of specific
27 diazotrophs were measured. Overall, nitrogen fixation rates were lower in the NSCS than
28 around the Luzon Strait and the western North Pacific, which we hypothesize was due to
29 lower Fe-to-fixed nitrogen supply ratios that decrease their competitive ability with non-
30 diazotrophic phytoplankton. The nutrient addition bioassay experiments demonstrated
31 that nitrogen fixation rates in the central northern South China Sea (NSCS) were co-
32 limited by Fe and P, whereas in the western boundary of the North Pacific they were P-
33 limited. Changes in the abundances of *nifH* in response to nutrient addition varied in how
34 well they correlated with changes in nitrogen fixation rates, and the largest responses
35 were always dominated by either *Trichodesmium* or UCYN-B. In general, nutrient
36 addition had a relatively restricted impact on diazotroph community structure apart from
37 on UCYN-B, which showed increased contribution to the diazotroph community



38 following P addition at sites where N₂ fixation rates were P-limited. We further
39 hypothesize the importance of absolute Fe supply rates in regulating spatial variability in
40 diazotroph community structure across the study area.



41 **1 Introduction**

42 Nitrogen fixation by diazotrophic bacteria converts abundant dinitrogen (N_2) gas into
43 ammonia, providing nearly half of the ocean's bioavailable nitrogen (N) (Gruber and
44 Galloway, 2008), which goes on to support >30% of carbon export from surface to deep
45 waters in the N-limited ocean (Böttjer et al., 2016; Wang et al., 2019). A diverse
46 community of diazotrophs has been described across the oligotrophic ocean that includes
47 *Trichodesmium*, unicellular cyanobacteria (UCYN-A and *Crocosphaera*, also referred to
48 as UCYN-B), the heterocystous symbiont *Richelia* associated with diatoms (DDAs,
49 diatom-diazotroph associations), and noncyanobacterial diazotrophs (NCDs,
50 heterotrophic or photoheterotrophic bacteria) (Zehr and Capone, 2020). However, there is
51 still a lack of knowledge on what controls diazotrophic distribution, activity and
52 community structure in the current ocean.

53

54 Iron (Fe) and phosphorus (P) are believed to be key factors controlling the biogeographic
55 distribution of marine N_2 fixation (Sohm et al., 2011; Zehr and Capone, 2020; Wen et al.,
56 2022). Fe is particularly important for N_2 fixers as a cofactor for the FeS-rich
57 nitrogenase enzyme (Berman-Frank et al., 2001), whereas P is also required for genetic
58 information storage, cellular structure and energy generation. A number of nutrient-
59 addition bioassay experiments conducted in the field have shown that N_2 fixation in the
60 oligotrophic oceans can be limited by Fe or P, or co-limited by both nutrients at the same



61 time (Mills et al., 2004; Needoba et al., 2007; Grabowski et al., 2008; Watkins-Brandt et
62 al., 2011; Langlois et al., 2012; Dekaezemacker et al., 2013; Krupke et al., 2015; Tanita et
63 al., 2021; Wen et al., 2022; Turk-Kubo et al., 2012). However, few studies have
64 quantified how the supply of Fe and/or P impacts the abundance of individual
65 diazotrophic phylotypes and their community structure (Langlois et al., 2012; Moisander
66 et al., 2012; Turk-Kubo et al., 2012). Experiments conducted so far that investigated this
67 were located in the South Pacific and North Atlantic, and found diverse responses among
68 diazotrophic phylotypes to the addition of Fe and/or P. Furthermore, the responses of total
69 diazotroph abundances assessed from *nifH* gene quantifications were not qualitatively
70 match the responses of bulk N₂ fixation rates (Langlois et al., 2012; Moisander et al.,
71 2012; Turk-Kubo et al., 2012). Resolution of the specific types of diazotrophs responding
72 to nutrient supply, in addition to overall N₂ fixation rates, are potentially crucial for
73 understanding their biogeography, which in turn could be important for biogeochemical
74 function. For example, the presence of large *Trichodesmium* filaments is expected to have
75 a different fate in the microbial food web and contribute differently to the sinking flux of
76 carbon than that of small unicellular species (Bonnet et al., 2016).

77

78 The northern South China Sea (NSCS) and the neighboring western boundary of the
79 North Pacific are interacting water bodies, with the major western boundary Kuroshio
80 Current intruding into the NSCS across the Luzon Strait, generating frontal zones with



81 unique physical and biogeochemical characteristics (Du et al., 2013; Guo et al., 2017;
82 Huang et al., 2019; Li et al., 2021; Lu et al., 2019; Xu et al., 2018). Common to the full
83 regime, however, is surface waters that are warm, stratified and N-depleted, but subject to
84 elevated dust input from the Gobi Desert (Duce et al., 1991; Jickells et al., 2005). These
85 conditions potentially provide an ideal habitat for diazotrophs (Chen et al., 2003; Wu et
86 al., 2003). Investigations in these regions have shown high variability in diazotroph
87 abundances and N₂ fixation rates (Chen et al., 2003; Chen et al., 2014; Chen et al., 2008;
88 Lu et al., 2019; Wu et al., 2018), which overall increased from the NSCS basin to the
89 western boundary of the North Pacific (Wen et al., 2022). Along this gradient in N₂
90 fixation, the dominant diazotroph types switched from *Trichodesmium* in the NSCS to
91 UCYN-B in the western boundary of the North Pacific (Wen et al., 2022). Several studies
92 have hypothesized that these gradients of diazotroph abundances and N₂ fixation rates
93 were regulated by nutrient availability (specifically, Fe, P and N; Wu et al., 2003; Chen et
94 al., 2003; Chen et al., 2008; Shiozaki et al., 2014a; Shiozaki et al., 2015a). More recent
95 observational and experimental evidence supported the hypothesis that Fe:N supply ratios
96 are the main drivers of the abundance of diazotrophs and N₂ fixation rates across the
97 western North Pacific (Wen et al., 2022). With an increasing supply ratio of Fe:N from
98 the North Equatorial Current (NEC) to the Philippines Sea, Wen et al. (2022) found that
99 diazotroph abundances and N₂ fixation rates increased, and bioassay experiments
100 demonstrated evidence for N₂ fixation rates switching from Fe to P limitation or to



101 nutrient-replete conditions. In the NSCS, Wen et al. (2022) found N_2 fixation rates fell in
102 between NEC and Kuroshio values and bioassay experiments demonstrated rates were
103 co-limited by Fe and P, which they hypothesized was due to intermediate Fe:N supply
104 ratios (Wen et al., 2022).

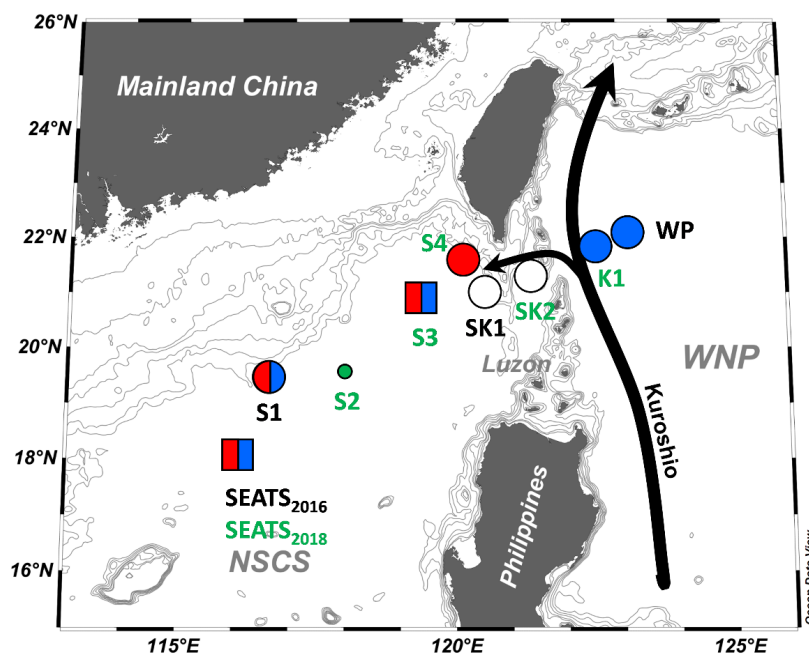
105

106 Although this previous study has outlined the broad spatial pattern of nutrient regulation
107 of marine N_2 fixation throughout the western Subtropical Pacific (Wen et al., 2022),
108 important questions remain. Two specific examples are: (i) the relatively lower spatial
109 resolution of the experiments in Wen et al. (2022) and other studies (Chen et al., 2019;
110 Shiozaki et al., 2014b) remain insufficient to delineate Fe and P controls at finer spatial
111 scales between the neighboring NSCS and the western boundary of the North Pacific; and
112 (ii) In addition to controls on N_2 fixation rates, broad-scale differences in the types of
113 diazotrophs dominating the N_2 fixer community were not concretely associated with
114 environmental drivers in experimental tests for nutrient limitation, because changes in
115 type-specific diazotroph abundances following nutrient addition were not measured
116 (Chen et al., 2019; Shiozaki et al., 2014b; Wen et al., 2022). Therefore, in the present
117 study we extend the findings of Wen et al. (2022) and others by carrying out additional,
118 higher-spatial resolution observations of volumetric N_2 fixation rates and measurements
119 of the abundances of key diazotrophic phylotypes from the NSCS basin to the western
120 boundary of the North Pacific (including the upstream Kuroshio) between 2016 and 2018



121 (Fig. 1). These new observations were supplemented by a further additional eight, high
122 volume (10 L) nutrient amendment bioassay experiments throughout the transect to
123 directly test the response of both (i) N_2 fixation rates, and (ii) *nifH* gene abundances to
124 supply of potentially limiting nutrients (Fe, P, and Fe+P).

125



126

127

128 **Figure 1.** Sampling and nutrient amendment experiment locations in the northern South
129 China Sea and the western boundary of the North Pacific. One station (SEATS₂₀₁₆) was
130 sampled in 2016, three (S1, SK1, WP) were in 2017, and six (stations with green labels)
131 were in 2018. Nutrient amendment experiments were conducted at 8 of 10 stations.
132 Symbols summarize the nutrient limitation of N_2 fixation rates found at each site: red, Fe
133 limitation; blue, P limitation; split red/blue, Fe-P co-limitation; white, nutrient replete.
134 Co-limitation type is indicated by symbol type (square, independent co-limitation; circle,
135 simultaneous co-limitation). WNP, the western North Pacific. Black arrows indicate
136 Kuroshio Current and its branch. Gray lines indicate 50, 100, 300, 500, 1000, 1500 and
137 2000 m bathymetric depth contours.



138

139 **2 Method**

140 **2.1 Sample collection**

141 Investigations and bioassay experiments were conducted on three cruises to the NSCS
142 (stations SETAS and S1 to S4), the Luzon Strait (stations SK1 and SK2), the upstream
143 Kuroshio (station K1), and the western boundary of the North Pacific (station WP) (Fig.
144 1), between May 2016 and June 2018 onboard the R/V *Dongfanghong 2* and R/V *Tan*
145 *Kah Kee*. At each station (except station SK2 where no hydrological data are available),
146 temperature and salinity were recorded by a Seabird 911 CTD. Water samples were
147 collected using Niskin-X bottles at five or six depths (except SK2, only surface waters
148 were sampled) throughout the upper 150 m for the determination of N₂ fixation and
149 primary production rates. Seawaters from each depth were also sampled for the analysis
150 of *nifH* gene abundance. Samples for nutrient analysis were also collected. Seawater for
151 the bioassay experiments (at 8 of 10 stations) was collected using a trace-metal-clean
152 towed sampling device located around 2-5 m depth with suction provided by a Teflon
153 bellows pump. Seawaters were sampled in a dedicated trace-metal-clean laminar flow
154 hood maintained over-pressurized by HEPA-filtered air. During the cruise in 2018
155 (stations with green labels in Fig. 1), surface waters were sampled under trace-metal-
156 clean condition for the determination of total particulate Fe concentration.

157



158 **2.2 N₂ fixation and primary production rate measurements**

159 N₂ fixation rates were determined by the ¹⁵N₂ gas dissolution method (Mohr et al., 2010),
160 combined with a primary production assay using NaH¹³CO₃ (99 atom% ¹³C, Cambridge
161 Isotope Laboratories). Briefly, 0.22 μm-filtered surface seawater was degassed using a
162 Sterapore membrane unit (20M1500A: Mitsubishi Rayon Co., Ltd., Tokyo, Japan) as
163 described in Shiozaki et al. (2015b). After that, 20 mL 98.9 atom% pure ¹⁵N₂ gas
164 (Cambridge Isotope Laboratories) was injected into a gas-tight plastic bag containing 2 L
165 of the degassed seawater and allowed to fully equilibrate before use. The N₂ fixation and
166 primary production incubations were conducted in duplicate 4.3 L Nalgene polycarbonate
167 bottles. Samples were spiked with 100 mL ¹⁵N₂ enriched filtered seawater from the same
168 site and incubated on-deck for 24 h. The final ¹⁵N₂ enriched seawater concentration in the
169 incubation bottles was not measured directly during this study. We thus employed a ¹⁵N₂
170 atom% of 1.40 ± 0.08 atom% (*n* = 17) measured in a following cruise in 2020 (Wen et al.,
171 2022), during which the N₂ fixation incubations were conducted using the same
172 approach, reagents, and equipment as for the study described here. For primary
173 production measurements, NaH¹³CO₃ solution was added at a concentration of 100 μM.
174 After that, the bottles were covered with a neutral-density screen to adjust the light to the
175 levels at sampling depths, and then were incubated for 24 h in an on-deck incubator
176 continuously flushed with surface seawater. Incubated samples were filtered onto pre-
177 combusted (450 °C, 4 h) GF/F filters, and the particulate organic matter from each depth



178 were also collected to determine background POC/PON concentrations and their natural
179 $^{13}\text{C}/^{15}\text{N}$ abundances.

180

181 All filter samples were acid fumed to remove the inorganic carbon and then analyzed
182 using an elemental analyzer coupled to a mass spectrometer (EA-IRMS, Thermo Fisher
183 Flash HT 2000-Delta V plus). The N_2 fixation and primary production rates were then
184 calculated according to Montoya et al. (1996) and Hama et al. (1983), respectively. The
185 detection limits of N_2 fixation rates were then calculated according to Montoya et al.
186 (1996), taking 4‰ as the minimum acceptable change in the $\delta^{15}\text{N}$ of particulate nitrogen.
187 All parameters involved in N_2 fixation rate calculation are shown in Supplementary
188 Materials. To represent the inventories, the upper 150 m depth-integrated N_2 fixation rate
189 and primary production were calculated by the trapezoidal integration method.

190

191 **2.3 *nifH* gene abundance**

192 At each depth, 4.3 L seawater samples for DNA extraction were filtered onto 0.22 μm
193 pore-sized membrane filters (Supor200, Pall Gelman, NY, USA) and then frozen in liquid
194 N_2 . To extract the DNA, membranes were cut into pieces under sterile conditions, and
195 then extracted using the QIAamp[®] DNA Mini Kit (Qiagen) following the manufacturer's
196 protocol. The quantitative polymerase chain reaction (qPCR) analysis was targeted on the
197 *nifH* phylotypes of *Trichodesmium* spp., unicellular cyanobacterial UCYN-A1, UCYN-



198 A2, and UCYN-B, *Richelia* spp. (het-1), and a gamma-proteobacterium (γ -24774A11),
199 using previously designed primers and probe sets (Supplementary Table S1; Church et al.,
200 2005a; Church et al., 2005b; Moisander et al., 2008; Thompson et al., 2014). A recent
201 study suggested that the primers for UCYN-A2 also target UCYN-A3 and thus cannot be
202 used to differentiate between these two phylotypes (Farnelid et al., 2016). Therefore, we
203 used the convention UCYN-A2/A3 when referring to these two groups. The *nifH*
204 standards were obtained by cloning the environmental sequences from previous samples
205 collected from the SCS. qPCR analysis was carried out as described previously (Church
206 et al., 2005a) with slight modifications. Triplicate qPCR reactions were run for each
207 environmental DNA sample and for each standard on a CFX96 Real-Time System (Bio-
208 Rad Laboratories). Standards corresponding to between 10^1 and 10^7 copies per well were
209 amplified in the same 96-well plate. The amplification efficiencies of PCR were always
210 between 90-105%, with R^2 values > 0.99 . The quantification limit of the qPCR reactions
211 was 10 *nifH* gene copies per reaction, and 1 μ L from 100 or 150 μ L template DNA was
212 applied to qPCR assay, which was equivalent to approximately ~ 230 -350 gene copies per
213 L of seawater sample filtered (4.3 L).

214

215 **2.4 Bioassay experiments**

216 Acid-cleaned Nalgene polycarbonate carboys (10 L) were filled with near surface

217 seawater from the towed fish system. Trace metal clean techniques were strictly applied



218 in experimental setup and manipulations. All materials coming in contact with the
219 incubation water were acid-washed in a Class-100 cleanroom before use. Nutrient
220 amendments at all sites were Fe, P, and Fe+P. The amended Fe and P (chelexed and filter-
221 sterilized) concentrations were 2 nM and 100 nM, respectively. Control bottles incubated
222 with no nutrient treatment were included in all experiments. All treatments were
223 conducted with 2 or 3 replicates and incubated for 3 days in a screened on-deck incubator
224 continuously flushed with surface seawater. After pre-incubation, subsamples were
225 collected for the determination of N₂ fixation rate and *nifH* gene abundance. ¹⁵N₂
226 enriched seawater was prepared as described above, except that all the materials coming
227 in contact with the seawater were acid-cleaned before use.

228

229 **2.5 Macronutrient and chlorophyll *a* analyses**

230 Samples for macronutrient analyses were collected in 125-mL acid-washed high-density
231 polyethylene (HDPE) bottles (Nalgene), and analyzed onboard using a Four-channel
232 Continuous Flow Technicon AA3 Auto-Analyzer (Bran-Lube GmbH). The detection
233 limits for NO₃⁻+NO₂⁻ and PO₄³⁻ were 0.1 μmol L⁻¹ and 0.08 μmol L⁻¹, respectively. The
234 nitracline was defined as the depth at which NO_x concentration equaled 0.1 μmol L⁻¹ (Le
235 Borgne et al., 2002). Samples for chlorophyll *a* analysis were collected on nominal 0.7
236 μm pore-size GF/F filters (Whatman) and chlorophyll *a* concentration was determined
237 using a Trilogy fluorometer (Turner-Designs, USA).



238

239 **2.6 Particulate Fe concentration**

240 Total particulate Fe (PFe_{total}) and intracellular Fe (PFe_{intra}) were sampled under laminar
241 flow hood. Briefly, 4-9 L of surface waters were filtered onto acid-cleaned 0.22- μ m
242 polycarbonate membrane filters. For PFe_{intra} samples, in order to remove metal-bound to
243 the cell surface, cells were exposed twice to an oxalate-EDTA solution for 5 minutes and
244 rinsed nine times with Chelex-cleaned 0.56 mol L⁻¹ NaCl solution (Li et al., 2020).
245 PFe_{total} and PFe_{intra} concentrations were then determined by ICP-MS (ICP-MS 7700X,
246 Agilent).

247

248 **2.7 Statistical analysis**

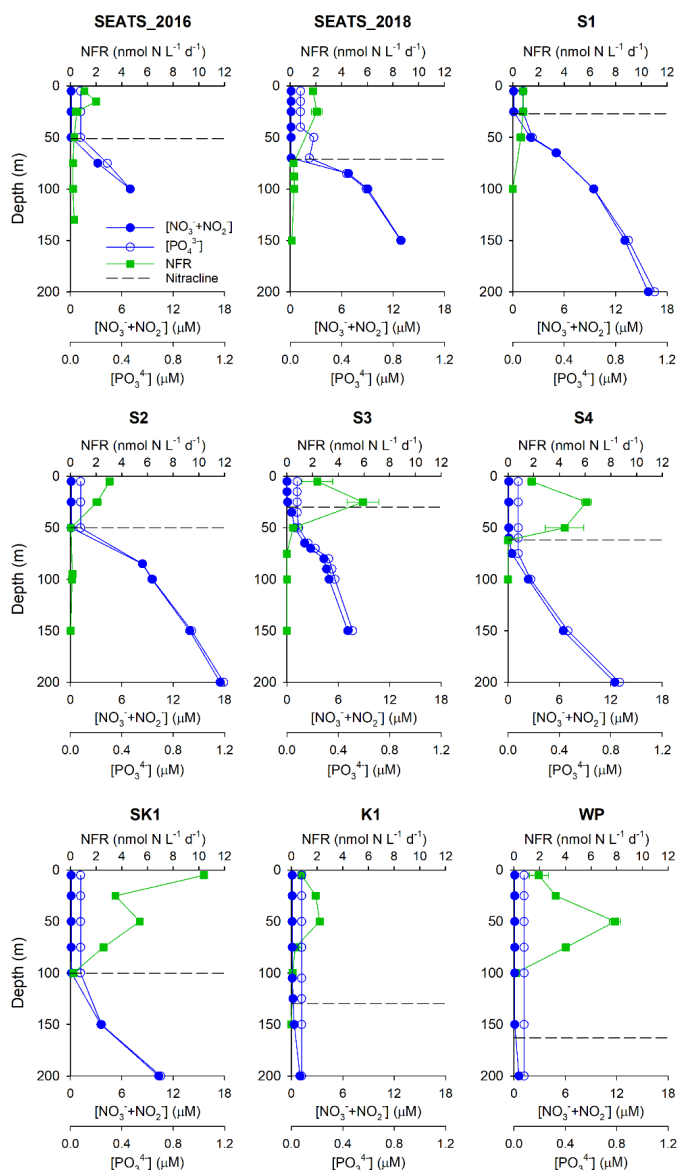
249 Significance of differences among nutrient treatments of bioassay experiments (for N₂
250 fixation rate) were tested by ANOVA followed by Fisher PSLD test, using R-4.1.2.
251 Pairwise correlation between N₂ fixation rates, diazotroph groups and environmental
252 factors was analyzed using Pearson correlation. A significance level of $p < 0.05$ was
253 applied, except as noted where significance was even greater.

254

255 **3 Results**

256 **3.1 Spatial variations of N₂ fixation rates and diazotroph composition**

257 Our survey revealed substantial spatial variability in N₂ fixation rates and *nifH* gene



258

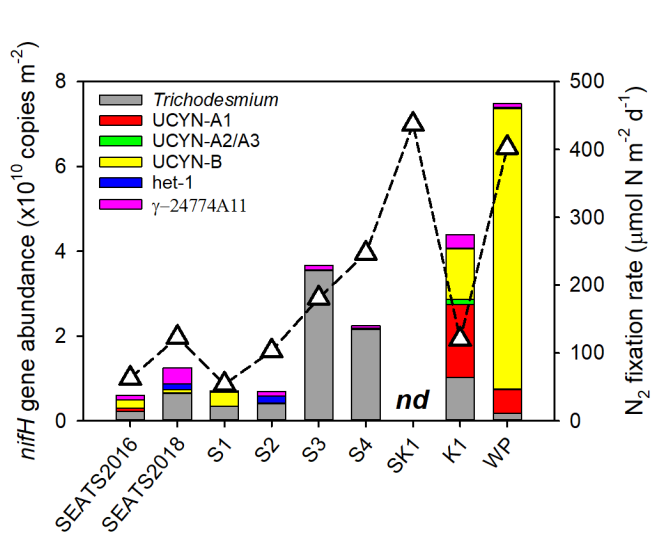
259

260 **Figure 2.** Vertical profiles of N₂ fixation rates. Green squares, N₂ fixation rate (NFR, nmol
261 N L⁻¹ d⁻¹); blue solid circles, NO₃⁻+NO₂⁻ concentrations (μM); blue open circles, PO₄³⁻
262 concentrations (μM). The dashed line indicates the nitracline depth. Note that no profile
263 data were available at station SK2.

264



265 abundances across the study area (Figs. 2 and 3). Vertically, high N₂ fixation rates were
266 found in the upper 50 m (ranged from below detection limit to 10.4 ± 0.01 nmol N L⁻¹ d⁻¹
267 ¹), rates dropped rapidly at greater depths (Fig. 2), and surface rates were positively
268 correlated with depth-integrated rates (Pearson $r = 0.68$, $p = 0.043$, Supplementary Table
269 S2). Horizontally, depth-integrated N₂ fixation rates were generally low at the central
270 NSCS basin stations (SEATS, S1 and S2, on average 86 ± 33 μmol N m⁻² d⁻¹), elevated at
271 stations close to the western edge of the Luzon Strait (S3 and S4, on average 214 ± 47 μmol
272 N m⁻² d⁻¹), and were highest at the Luzon Strait station (SK1, 437 μmol N m⁻² d⁻¹) and the
273 western North Pacific boundary station (WP, 403 μmol N m⁻² d⁻¹) (Figs. 1, 3 and Table 1).
274



275
276
277
278
279

Figure 3. Depth-integrated (upper 150 m) *nifH* gene abundances (bars) and N₂ fixation rates (triangles). Note that depth-integrated N₂ fixation rates and *nifH* gene abundances were not available at station SK2. nd, not determined.



280

281 **Table 1.** Environmental conditions, N₂ fixation, and primary production rates. Sea
282 surface temperature (SST) and salinity (SSS), nitracline depth (D_{Nitr}), surface N₂ fixation
283 rate (SNF), upper 150 m depth-integrated N₂ fixation rate (INF) and primary production
284 (IPP) at each station. nd, not determined.

Station	SST (°C)	SSS	Chl <i>a</i> (µg/L)	D _{Nitr} (m)	SNF (nmol N L ⁻¹ d ⁻¹)	INF (µmol N m ⁻² d ⁻¹)	IPP (mmol C m ⁻² d ⁻¹)
SEATS ₂₀₁₆	30.3	33.46	0.26	51	1.1	63	44
SEATS ₂₀₁₈	30.3	33.46	0.11	71	1.8	123	24
S1	29.5	33.73	0.24	27	0.8	54	43
S2	29.4	33.75	0.10	50	3.0	103	24
S3	28.7	33.53	0.15	30	2.4	181	98
S4	29.5	33.74	0.17	62	1.8	247	59
SK1	30.5	33.62	0.22	100	10.4	437	11
SK2	nd	nd	0.11	nd	2.0	nd	nd
K1	29.1	34.45	0.11	130	0.8	120	19
WP	30.9	34.47	0.11	163	1.9	403	9

285

286 A significant positive correlation was found between the depth-integrated *nifH* gene
287 abundance and N₂ fixation rate (Pearson $r = 0.72$, $p = 0.046$, Supplementary Table S2),
288 demonstrating that the abundances of these major diazotroph phylotypes well explained
289 the major variability in measured rates. However, considerable spatial variation was
290 found in the specific diazotrophs supporting N₂ fixation (Fig. 3). *Trichodesmium*



291 dominated the diazotroph assemblage throughout the water column of the NSCS (52-96%
292 of the total *nifH* gene abundance, excluding station SEATE₂₀₁₆). In contrast, at the
293 Kuroshio station K1, unicellular diazotrophic cyanobacteria (UCYN-A and UCYN-B)
294 were the most abundant phylotypes, and at station WP, UCYN-B alone was dominant
295 (Fig. 3 and Supplementary Table S3).

296

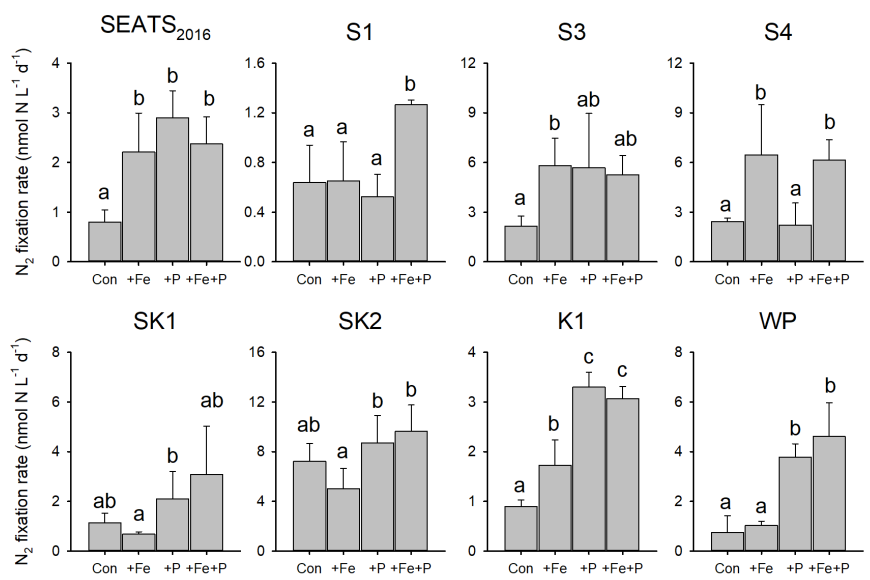
297 **3.2 Diazotroph response to Fe and P supply**

298 To directly test which nutrients were limiting overall N₂ fixation rates and the abundance
299 of individual diazotrophs, we conducted eight, ~3-day nutrient addition bioassay
300 experiments (Figs. 4 and 5). The responses of N₂ fixation rate to different combinations
301 of Fe and P supply demonstrated a coherent geographic switch across the study area
302 (Figs. 1, 4 and 5). At stations towards to the NSCS basin (SEATS₂₀₁₆, S1 and S3), N₂
303 fixation rates were co-limited by Fe and P. Two forms of this co-limitation were
304 identified: (i) only simultaneous Fe and P addition stimulated N₂ fixation rates
305 ('simultaneous co-limitation', station S1, Fig. 4); (ii) independent addition of either Fe or
306 P alone, or supply of Fe and P in combination, enhanced N₂ fixation rates ('independent
307 co-limitation', stations SEATS₂₀₁₆ and S3, Fig 4). Further to the northeast, in contrast, N₂
308 fixation rates were only stimulated by nutrient combinations containing Fe at S4 and by
309 combinations containing P at K1 and WP, suggesting single limitation by Fe or P,
310 respectively, at these sites (Fig. 4). Although Fe addition also appeared to stimulate N₂



311 fixation rates at station K1, P was generally the major limiting nutrient at this station
312 taking into account the responses of both N_2 fixation rates and *nifH* gene abundance (see
313 below) (Figs. 4 and 5). At stations (SK1 and SK2) in the Luzon Strait, mean N_2 fixation
314 rates were highest in treatments containing P, but responses were not significantly greater
315 than the untreated controls, suggesting that both Fe and P availability were not limiting
316 N_2 fixation rates (Fig. 4).

317



318

319

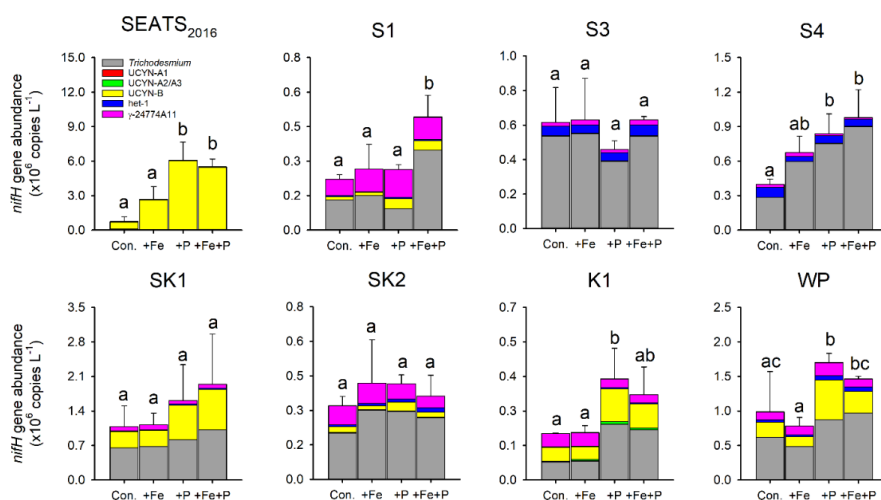
320 **Figure 4.** Response of N_2 fixation to nutrient amendment. Error bars represent the standard
321 deviation of biological replicates ($n = 2$ or 3). Different letters above error bars indicate
322 statistically significant differences ($p < 0.05$) between treatments (ANOVA followed by
323 Fisher PLSD test).

324

325 Further detail as to the drivers of the N_2 fixation responses to Fe and P additions was



326 provided by the species-level analysis of diazotroph *nifH* from the treatment bottles. In
 327 general, responses of total *nifH* gene abundance to Fe and P amendments were
 328 qualitatively consistent with N₂ fixation rates at most sites, that is, the nutrient(s) limiting
 329 N₂ fixation rates also limited the diazotroph abundance (Figs. 4 and 5). The exceptions
 330 were at stations S3 and S4, where variability in *nifH* abundances was observed in
 331 response to nutrient treatment (station S3) or overall trends differed between *nifH*
 332 abundances and N₂ fixation rates (station S4; enhanced *nifH* abundance in response to +P,
 333 whereas rates only responded to +Fe). Quantitatively, the responses of N₂ fixation
 334



335
 336
 337 **Figure 5.** Response of diazotroph phylotypes to nutrient amendment. Bar heights
 338 represent the mean total *nifH* concentration and error bars the standard deviation of
 339 biological replicates ($n = 2$ or 3). Different letters above error bars indicate a statistically
 340 significant difference ($p < 0.05$) between treatments (ANOVA followed by Fisher PLSD
 341 test).

342



343 rates and *nifH* biomass to nutrient addition were not well correlated (total *nifH* abundance
344 increase rate versus N₂ fixation increase rate following nutrient supply, $R^2 = 0.07$, $p =$
345 0.21; Supplementary Fig. S1), despite initial background *nifH* abundances and N₂ fixation
346 rates being well correlated (Pearson $r = 0.72$, $p = 0.046$, Supplementary Table S1). This
347 suggested a decoupling of the rates of change in biomass and N₂ fixation rates following
348 nutrient addition over the relative short incubation timescales (~3 days).

349

350 Overall, the diazotroph community structure was not greatly changed after nutrient
351 amendments (Fig. 5). *Trichodesmium* and UCYN-B were the two most dominant species
352 in all experimental waters that contributed to the enhanced total *nifH* gene abundance
353 after nutrient additions (Figs. 3, 5 and Supplementary Fig. S1). Despite showing
354 independent co-limitation in response to Fe and P supply at station SEATS₂₀₁₆ (Fig. 4), as
355 reflected by equally responding N₂ fixation rates, UCYN-B, the dominant diazotroph in
356 non-amended control waters, increased 2-fold more following P addition in comparison
357 to Fe addition (Fig. 5 and Supplementary Fig. S2). Furthermore, no significant changes in
358 *nifH* were observed at station S3, where N₂ fixation rates were also independently Fe-P
359 co-limited. More consistent between the N₂ fixation rates and *nifH* biomass changes were
360 the *nifH* responses at station S1, with overall *nifH* concentrations only responding to
361 Fe+P additions, matching the N₂ fixation response. This was mostly driven by co-
362 limitation of *Trichodesmium*, whereas UCYN-B responded only to P supply (Fig. 5 and



363 Supplementary Fig. S2).

364

365 In contrast to the Fe limitation of N₂ fixation rates found at station S4, *nifH* abundances
366 showed the most significant responses to the combined supply of Fe and P. However, at
367 sites where N₂ fixation rates were P-limited (K1 and WP) overall *nifH* concentrations also
368 responded most to P addition, with contributions from both *Trichodesmium* and UCYN-B
369 (Fig. 5). In addition, *het-1* also increased significantly with +P combinations at stations
370 K1 and WP (Supplementary Fig. S2). By contrast, γ -24774A11, which also accounted for
371 a substantial fraction of the diazotroph community (up to 31%), did not show clear
372 enhancement to nutrient additions (Supplementary Fig. S2), suggesting that it was not Fe-
373 and/or P-limited.

374

375 **4 Discussion**

376 In the present study, rates and *nifH* gene abundances were much higher in the northeast
377 region of our study area than in the NSCS basin (Fig. 3). Rates at stations SK1 and WP
378 were comparable to those recently reported in this region ($\sim 450 \mu\text{mol N m}^{-2} \text{d}^{-1}$)
379 measured using the same ¹⁵N₂ gas dissolution method (Lu et al., 2019; Wen et al., 2022).
380 Although relatively low rates were measured at the Kuroshio Current station (K1)
381 compared with previous observations (e.g., Wen et al., 2022), high *nifH* gene abundance
382 was nevertheless observed at this site (Fig. 3 and Supplementary Table S3). Therefore,



383 our observations provide increasing evidence for this western (sub)tropical North Pacific
384 boundary region containing important “hot spots” of N₂ fixation (Shiozaki et al., 2010;
385 Shiozaki et al., 2015a; Wen et al., 2022). However, the elevated total *nifH* concentration
386 in the western boundary of the North Pacific during our study was largely attributed to an
387 increased abundance of unicellular diazotrophs (UCYN-A and B, Fig. 3), but not
388 *Trichodesmium* as previously reported (Chen et al., 2003; Chen et al., 2014; Chen et al.,
389 2008; Shiozaki et al., 2014a). Instead, we found that *Trichodesmium* was most abundant
390 at stations (S3 and S4) close to the western edge of the Luzon Strait (Fig. 3 and
391 Supplementary Table S3), where Kuroshio intrusion water has been hypothesized to
392 introduce *Trichodesmium* into a favorable biogeographic regime (Lu et al., 2019). Either
393 this region is spatially and/or temporally heterogeneous with respect to the presence of
394 unicellular versus *Trichodesmium* diazotrophs, or the environmental changes have led to
395 a shift in diazotroph community structure (Gruber, 2011; Hutchins and Fu, 2017).
396
397 Depth-integrated N₂ fixation rate and *nifH* gene abundance were not correlated with sea
398 surface temperature (SST), but a significant positive correlation was found between
399 nitracline depth and total *nifH* gene abundance (Pearson $r = 0.74$, $p = 0.037$,
400 Supplementary Table S2). This was suggestive of subsurface N supply into the euphotic
401 zone, which is inversely related to nitracline depth, potentially being important in
402 regulating diazotroph abundance in our study area, with lower N supply leading to



403 enhanced diazotroph abundances (Chen et al., 2003; Shiozaki et al., 2014b). The presence
404 of diazotrophs in the ocean will be a function of how well they can compete with non-
405 diazotrophic phytoplankton for limiting resources (e.g., Fe and P) under grazing pressure
406 (Dutkiewicz et al., 2014; Landolfi et al., 2021; Ward et al., 2013). Accordingly, because
407 of the growth characteristics of diazotrophs in comparison to non-diazotrophs, in
408 particular their lack of requirement for pre-fixed N, but higher requirement for Fe and P,
409 the relative supply rates of N, Fe and P are highly important in dictating where
410 diazotrophs can succeed (Ward et al., 2013). Aligning with earlier global model
411 predictions (Ward et al., 2013), and investigations in the (sub)tropical Atlantic (Schlosser
412 et al., 2014), Wen et al. (2022) recently found that the Fe:N supply ratio (including
413 subsurface and aerosol N and Fe supplies) was a robust predictor of diazotroph standing
414 stock across the broader western North Pacific, including our study region.

415

416 Although the current study lacked the data to calculate nutrient supply rates into the
417 euphotic zone (matching Fe concentration profiles, euphotic depths), the correlation
418 found between *nifH* and nitracline depth suggested the potential for the same driver (i.e.,
419 Fe:N supply rates) to be operating over this smaller spatial scale. In line with Wen et al.
420 (2022), we further hypothesize that the expected significant N supply rate to surface
421 waters of the NSCS (due to a shallower nitracline, alongside riverine and aerosol inputs)
422 reduces, but does not eliminate the competitive ability of diazotrophs, as Fe supply rates



423 to this region are likely also high (Duce et al., 1991; Jickells et al., 2005; Zhang et al.,
424 2019), thereby maintaining Fe:N supply ratios at levels supporting diazotrophs (Ward et
425 al., 2013; Wen et al., 2022). At these Fe:N supply levels, we observed that N₂ fixation
426 rates were either (i) ‘simultaneously co-limited’ by Fe and P (identified at station S1),
427 which represents a state where two, non-substitutable nutrients (in this case, Fe and P)
428 have been drawn down to equally limiting levels (Sperfeld et al., 2016), or (ii)
429 ‘independently co-limited’ (stations SEATS₂₀₁₆ and S3), which represents a state where
430 the resources are substitutable at biogeochemical (Saito et al., 2008), or community levels
431 (Arrigo, 2005).

432

433 The measured contributions of individual diazotrophs to total *nifH* concentration in
434 response to nutrient supply suggested that simultaneous Fe-P co-limitation of N₂ fixation
435 rates at station S1 was via regulation of *Trichodesmium*, which only responded to Fe+P
436 addition (Fig. 5). The *nifH* responses also suggested that independent Fe-P co-limitation
437 of N₂ fixation rates at sites SEATS₂₀₁₆ and S3 was not operating at the community level
438 (i.e., one diazotroph type limited by Fe and the other by P) (Arrigo, 2005), as different
439 diazotroph community structure responses to either Fe or P addition were not observed
440 (Fig. 5). We suggest three possible causes for this observation: (i) co-limitation was at the
441 biochemical rather than community level (i.e., either Fe or P could enhance the rates of
442 processes ultimately driving elevated N₂ fixation) (Saito et al., 2008); (ii) a more subtle



443 community co-limitation was occurring at the level of ecotypes not resolved by the *nifH*
444 qPCR analyses; or (iii) community co-limitation of N₂ fixation rates for the measured
445 groups was occurring, but, unlike the simultaneous co-limitation scenario at station S1,
446 experimental durations were too short for this to be reflected in diazotroph biomass
447 changes. Surprisingly, stations with independent co-limitation of N₂ fixation rates by Fe
448 and P (SEATS₂₀₁₆ and S3) were not additive (i.e., increases in N₂ fixation rates in Fe+P
449 treatments were not larger than Fe and P alone) (Sperfeld et al., 2016). Although the
450 available data do not allow us to provide a concrete reason for this, it could reflect serial
451 limitation of N₂ fixation by another resource (e.g., a different nutrient or light).

452

453 In contrast to the more central NSCS, in the western boundary of the North Pacific,
454 elevated Fe:N supply ratios are expected as a result of deepening nitraclines (Fig. 2 and
455 Table 1) and continued aerosol Fe inputs (Wen et al., 2022). Additional Fe inputs other
456 than aerosol deposition may have also contributed to further enhanced Fe:N supply in the
457 Luzon Strait. At station SK2, much higher surface particulate Fe concentrations (both
458 intracellular and total forms) were observed (Supplementary Table S4), implying
459 additional Fe inputs, potentially sourced from the adjacent islands and the surrounding
460 shallow sub-surface bathymetry (Shiozaki et al., 2014a; Shiozaki et al., 2015a). In turn
461 we hypothesize that elevated Fe:N supply rates enhance N₂ fixation rates at these sites
462 (Fig. 3), which leads to P drawdown and subsequent P limitation of the enhanced



463 diazotroph stock (Figs. 4 and 5; Hashihama et al., 2009; Ward et al., 2013; Wen et al.,
464 2022).

465

466 In addition to the Fe:N supply ratio regulating the total *nifH* gene abundance and activity
467 (Wen et al., 2022), we also further hypothesize that overall Fe supply rates might be an
468 important factor in determining the diazotroph community structure in our study area
469 (Church et al., 2008; Langlois et al., 2008; Shiozaki et al., 2017). Specifically, the depth-
470 integrated diazotroph compositions switched from being co-dominated by *Trichodesmium*
471 and other diazotrophs in the central NSCS (SEATS, S1 and S2), *Trichodesmium*-
472 dominated in the more northern NSCS (S3 and S4), and finally dominated by UCYN-B in
473 the western boundary of the North Pacific (Fig. 3 and Supplementary Table S3). Elevated
474 Fe supply in the NSCS, particularly around the islands and shallow bathymetry of the
475 Luzon Strait, might create a more favorable condition for *Trichodesmium* (Fig. 3 and
476 Supplementary Table S3), consistent with elevated Fe demands of this species (Kupper et
477 al., 2008; Sohm et al., 2011), as well as its ability to use particulate Fe forms (Rubin et
478 al., 2011), and in line with the elevated contribution of this species found in other regions
479 with enhanced Fe supply (e.g., the tropical North Atlantic and western South Pacific;
480 Bonnet et al. 2018; Sañudo-Wilhelmy et al., 2001; Sohm et al., 2011; Stenegren et al.,
481 2018). Conversely, unicellular species may be more competitive than *Trichodesmium* in
482 regions with lower Fe supply rates (Fig. 3). In addition to having a higher surface to



483 volume ratio that favors Fe uptake (Hudson and Morel 1990; Jacq et al., 2014), UCYN-B
484 species such as *Crocospaera* have been reported to employ a repertoire of Fe-
485 conservation strategies, e.g., daily synthesis and breakdown of metalloproteins to recycle
486 Fe between the photosynthetic and N₂ fixation metalloenzymes and increased expression
487 of flavodoxin at night even under Fe-replete conditions (Saito et al., 2011). These
488 potentially explain why UCYN-B was less Fe-limited in the NSCS basin (stations
489 SEATS₂₀₁₆ and S1; Fig. 5 and Supplementary Fig. S2) and dominates the diazotroph
490 community on the western Pacific side of the Luzon Strait (Fig. 3; Chen et al., 2019; Wen
491 et al., 2022).

492

493 **5 Conclusions**

494 Observations and experiments conducted in the NSCS and the western boundary of the
495 North Pacific demonstrated that in the more central NSCS, Fe and P were co-limiting the
496 lower overall observed N₂ fixation rates, whereas P was limiting the higher rates on the
497 western Pacific side of the Luzon Strait. This matched the expectation of higher Fe:N
498 supply ratios in the western Pacific generating a more favorable niche for diazotrophs,
499 leading to a drawdown of P. *Trichodesmium* and UCYN-B were the most dominant
500 diazotroph types in the incubation waters and both dominated the responses of the total
501 *nifH* gene after nutrient amendments. In general, nutrient addition had a relatively
502 restricted impact on diazotroph community structure apart from on UCYN-B, which



503 showed increased contribution in the diazotroph community following P addition at sites
504 where N₂ fixation rates were P-limited. We hypothesize that overall switches in
505 diazotroph community structure from *Trichodesmium*-dominated in the NSCS to single-
506 celled UCYNA/B was related to declines in overall Fe supply rates and the different
507 physiological strategies of these diazotrophs to obtain and use Fe. Future research that
508 more accurately constrains nutrient supply rates to these different regions would be
509 beneficial for further resolving this hypothesis.



510 *Data availability.* All data needed to evaluate the conclusions in the paper are present in
511 the paper and/or the Supplementary Materials. Additional data associated with the paper
512 are available from the corresponding authors upon request.

513

514 *Author contributions.* D.S., H.H., and Z.W. designed the research. Z.W., R.D., W.W.,
515 W.L., X.H., W.L., and L.W. performed the experiments. Z.W., D.S., H.H., T.J.B., X.L.,
516 and Z.C. analyzed the data. Z.W., T.J.B., H.H., and D.S. wrote the manuscript. All authors
517 discussed the results and commented and edited the manuscript.

518

519 *Competing interests.* The authors declare that they have no conflict of interest.

520

521 *Acknowledgements.* The authors acknowledge the captains and crew of the R/V
522 *Dongfanghong 2* and R/V *Tan Kah Kee* for the help during the cruises. This work was
523 supported by the National Science Foundation of China (41890802, 42076149,
524 41925026, 42106041, and 41721005), the “111” Project (BP0719030), and the
525 XPLORER Prize from the Tencent Foundation to D. Shi.



526 **References**

- 527 Arrigo, K. R.: Marine microorganisms and global nutrient cycles, *Nature*, 437, 349-355,
528 10.1038/nature04158, 2005.
- 529 Berman-Frank, I., Cullen, J. T., Shaked, Y., Sherrell, R. M., and Falkowski, P.: Iron
530 availability, cellular iron quotas, and nitrogen fixation in *Trichodesmium*, *Limnol.*
531 *Oceanogr.*, 46, 1249-1260, 10.4319/lo.2001.46.6.1249, 2001.
- 532 Bonnet, S., Baklouti, M., Gimenez, A., Berthelot, H., and Berman-Frank, I.:
533 Biogeochemical and biological impacts of diazotroph blooms in a low-nutrient, low-
534 chlorophyll ecosystem: synthesis from the VAHINE mesocosm experiment (New
535 Caledonia), *Biogeosciences*, 13, 4461-4479, 10.5194/bg-13-4461-2016, 2016.
- 536 Bonnet, S., Caffin, M., Berthelot, H., Grosso, O., Benavides, M., Helias-Nunige, S., Guieu,
537 C., Stenegren, M., and Foster, R. A.: In-depth characterization of diazotroph activity
538 across the Western Tropical South Pacific hot spot of N₂ fixation (OUTPACE cruise),
539 *Biogeosciences*, 15, 4215-4232, 10.5194/bg-15-4215-2018 2018.
- 540 Böttjer, D., Dore, J. E., Karl, D. M., Letelier, R. M., Mahaffey, C., Wilson, S. T., Zehr, J.
541 P., and Church, M. J.: Temporal variability of nitrogen fixation and particulate
542 nitrogen export at Station ALOHA, *Limnol. Oceanogr.*, 62, 200-216,
543 10.1002/lno.10386, 2016.
- 544 Chen, M., Lu, Y., Jiao, N., Tian, J., Kao, S. J., and Zhang, Y.: Biogeographic drivers of
545 diazotrophs in the western Pacific Ocean, *Limnol. Oceanogr.*, 64, 1403-1421,



- 546 10.1002/lno.11123, 2019.
- 547 Chen, Y. L. L., Chen, H. Y., and Lin, Y. H.: Distribution and downward flux of
548 *Trichodesmium* in the South China Sea as influenced by the transport from the
549 Kuroshio Current, Mar. Ecol. Prog. Ser., 259, 47-57, 10.3354/meps259047, 2003.
- 550 Chen, Y. L. L., Chen, H. Y., Tuo, S. H., and Ohki, K.: Seasonal dynamics of new production
551 from *Trichodesmium* N₂ fixation and nitrate uptake in the upstream Kuroshio and
552 South China Sea basin, Limnol. Oceanogr., 53, 1705-1721,
553 10.4319/lo.2008.53.5.1705, 2008.
- 554 Chen, Y. L. L., Chen, H. Y., Lin, Y. H., Yong, T. C., Taniuchi, Y., and Tuo, S. H.: The relative
555 contributions of unicellular and filamentous diazotrophs to N₂ fixation in the South
556 China Sea and the upstream Kuroshio, Deep Sea Research Part I, 85, 56-71,
557 10.1016/j.dsr.2013.11.006, 2014.
- 558 Church, M. J., Björkman, K., and Karl, D.: Regional distributions of nitrogen-fixing
559 bacteria in the Pacific Ocean, Limnol. Oceanogr., 53, 63-77, 2008.
- 560 Church, M. J., Jenkins, B. D., Karl, D. M., and Zehr, J. P.: Vertical distributions of nitrogen
561 fixing phylotypes at Stn ALOHA in the oligotrophic North Pacific Ocean, Aquat.
562 Microb. Ecol., 38, 3-14, 10.3354/ame038003 2005a.
- 563 Church, M. J., Short, C. M., Jenkins, B. D., Karl, D. M., and Zehr, J. P.: Temporal patterns
564 of nitrogenase gene (*nifH*) expression in the oligotrophic North Pacific Ocean, Appl.
565 Environ. Microbiol., 71, 5362-5370, 10.1128/AEM.71.9.5362-5370.2005, 2005b.



- 566 Dekaezemacker, J., Bonnet, S., Grosso, O., Moutin, T., Bressac, M., and Capone, D. G.:
567 Evidence of active dinitrogen fixation in surface waters of the eastern tropical South
568 Pacific during El Niño and La Niña events and evaluation of its potential nutrient
569 controls, *Global Biogeochem. Cycles*, 27, 768-779, 10.1002/gbc.20063, 2013.
- 570 Du, C., Liu, Z., Dai, M., Kao, S. J., Cao, Z., Zhang, Y., Huang, T., Wang, L., and Li, Y.:
571 Impact of the Kuroshio intrusion on the nutrient inventory in the upper northern
572 South China Sea: Insights from an isopycnal mixing model, *Biogeosciences*, 10,
573 6419-6432, 10.5194/bg-10-6419-2013, 2013.
- 574 Duce, R. A., Liss, P. S., Merrill, J. T., Atlas, E. L., Buat-Menard, P., Hicks, B. B., Miller, J.
575 M., Prospero, J. M., Arimoto, R., Church, T. M., Ellis, W., Galloway, J. N., Hansen,
576 L., Jickells, T. D., Knap, A. H., Reinhardt, K. H., Schneider, B., Soudine, A., Tokos,
577 J. J., Tsunogai, S., Wollast, R., and Zhou, M.: The atmospheric input of trace species
578 to the world ocean, *Global Biogeochem. Cycles*, 5, 193-259, 10.1029/91gb01778,
579 1991.
- 580 Dutkiewicz, S., Ward, B. A., Scott, J., and Follows, M. J.: Understanding predicted shifts
581 in diazotroph biogeography using resource competition theory, *Biogeosciences*, 11,
582 5445-5461, 10.5194/bg-11-5445-2014, 2014.
- 583 Farnelid, H., Turk-Kubo, K., Muñoz-Marín, M. C., and Zehr, J. P.: New insights into the
584 ecology of the globally significant uncultured nitrogen-fixing symbiont UCYN-A,
585 *Aquat. Microb. Ecol.*, 77, 125-138, 10.3354/ame01794, 2016.



- 586 Grabowski, M. N. W., Church, M. J., and Karl, D. M.: Nitrogen fixation rates and controls
587 at Stn ALOHA, *Aquat. Microb. Ecol.*, 52, 175-183, 10.3354/ame01209, 2008.
- 588 Gruber, N.: Warming up, turning sour, losing breath: ocean biogeochemistry under global
589 change, *Philos T R Soc A*, 369, 1980-1996, 10.1098/rsta.2011.0003, 2011.
- 590 Gruber, N. and Galloway, J. N.: An Earth-system perspective of the global nitrogen cycle,
591 *Nature*, 451, 293-296, 10.1038/nature06592, 2008.
- 592 Guo, L., Xiu, P., Chai, F., Xue, H. J., Wang, D. X., and Sun, J.: Enhanced chlorophyll
593 concentrations induced by Kuroshio intrusion fronts in the northern South China Sea,
594 *Geophys. Res. Lett.*, 44, 11565-11572, 10.1002/2017GL075336, 2017.
- 595 Hama, T., Miyazaki, T., Ogawa, Y., Iwakuma, T., Takahashi, M., Otsuki, A., and Ichimura,
596 S.: Measurement of photosynthetic production of a marine phytoplankton population
597 using a stable ^{13}C isotope., *Mar. Biol.*, 73, 31-36, 10.1007/BF00396282 1983.
- 598 Hashihama, F., Furuya, K., Kitajima, S., Takeda, S., Takemura, T., and Kanda, J.: Macro-
599 scale exhaustion of surface phosphate by dinitrogen fixation in the western North
600 Pacific, *Geophys. Res. Lett.*, 36, L03610, 10.1029/2008gl036866, 2009.
- 601 Huang, Y., Laws, E. A., Chen, B., and Huang, B.: Stimulation of heterotrophic and
602 autotrophic metabolism in the mixing zone of the Kuroshio Current and northern
603 South China Sea: Implications for export production, *Journal of Geophysical*
604 *Research: Biogeosciences*, 124, 2645-2661, 10.1029/2018jg004833, 2019.
- 605 Hudson, R. J. M. and Morel, F. M. M.: Iron transport in marine-phytoplankton - kinetics of



606 cellular and medium coordination reactions, *Limnol. Oceanogr.*, 35, 1002-1020,
607 10.4319/lo.1990.35.5.1002, 1990.

608 Hutchins, D. A. and Fu, F.: Microorganisms and ocean global change, *Nature microbiology*,
609 2, 17058, 10.1038/nmicrobiol.2017.58, 2017.

610 Jacq, V., Ridame, C., L'Helguen, S., Kaczmar, F., and Saliot, A.: Response of the unicellular
611 diazotrophic cyanobacterium *Crocospaera watsonii* to iron limitation, *PLoS One*, 9,
612 e86749, 10.1371/journal.pone.0086749, 2014.

613 Jickells, T. D., An, Z. S., Andersen, K. K., Baker, A. R., Bergametti, G., Brooks, N., Cao,
614 J. J., Boyd, P. W., Duce, R. A., Hunter, K. A., Kawahata, H., Kubilay, N., laRoche, J.,
615 Liss, P. S., Mahowald, N., Prospero, J. M., Ridgwell, A. J., Tegen, I., and Torres, R.:
616 Global iron connections between desert dust, ocean biogeochemistry, and climate,
617 *Science*, 308, 67-71, 10.1126/science.1105959, 2005.

618 Krupke, A., Mohr, W., LaRoche, J., Fuchs, B. M., Amann, R. I., and Kuypers, M. M.: The
619 effect of nutrients on carbon and nitrogen fixation by the UCYN-A-haptophyte
620 symbiosis, *Isme J*, 9, 1635-1647, 10.1038/ismej.2014.253, 2015.

621 Kupper, H., Setlik, I., Seibert, S., Prasil, O., Setlikova, E., Strittmatter, M., Levitan, O.,
622 Lohscheider, J., Adamska, I., and Berman-Frank, I.: Iron limitation in the marine
623 cyanobacterium *Trichodesmium* reveals new insights into regulation of
624 photosynthesis and nitrogen fixation, *New Phytol.*, 179, 784-798, 10.1111/j.1469-
625 8137.2008.02497.x, 2008.



- 626 Landolfi, A., Prowe, A. E. F., Pahlow, M., Somes, C. J., Chien, C. T., Schartau, M., Koeve,
627 W., and Oschlies, A.: Can top-down controls expand the ecological niche of marine
628 N₂ fixers?, *Front Microbiol*, 12, 690200, 10.3389/fmicb.2021.690200, 2021.
- 629 Langlois, R. J., Hummer, D., and LaRoche, J.: Abundances and distributions of the
630 dominant *nifH* phylotypes in the Northern Atlantic Ocean, *Appl. Environ. Microbiol.*,
631 74, 1922-1931, 10.1128/AEM.01720-07, 2008.
- 632 Langlois, R. J., Mills, M. M., Ridame, C., Croot, P., and LaRoche, J.: Diazotrophic bacteria
633 respond to Saharan dust additions, *Mar. Ecol. Prog. Ser.*, 470, 1-14,
634 10.3354/meps10109, 2012.
- 635 Le Borgne, R., Barber, R. T., Delcroix, T., Inoue, H. Y., Mackey, D. J., and Rodier, M.:
636 Pacific warm pool and divergence: Temporal and zonal variations on the equator and
637 their effects on the biological pump, *Deep Sea Research Part II*, 49, 2471-2512,
638 10.1016/S0967-0645(02)00045-0, 2002.
- 639 Li, W., Sunda, W. G., Lin, W., Hong, H., and Shi, D.: The effect of cell size on cellular Zn
640 and Cd and Zn-Cd-CO₂ colimitation of growth rate in marine diatoms, *Limnol.*
641 *Oceanogr.*, 65, 2896-2911, 10.1002/lno.11561, 2020.
- 642 Li, X., Wu, K., Gu, S., Jiang, P., Li, H., Liu, Z., and Dai, M.: Enhanced biodegradation of
643 dissolved organic carbon in the western boundary Kuroshio Current when intruded
644 to the marginal South China Sea, *J Geophys Res-Oceans*, 126, e2021JC017585,
645 10.1029/2021jc017585, 2021.



- 646 Lu, Y., Wen, Z., Shi, D., Lin, W., Bonnet, S., Dai, M., and Kao, S. J.: Biogeography of N₂
647 fixation influenced by the western boundary current intrusion in the South China Sea,
648 J Geophys Res-Oceans, 124, 6983-6996, 10.1029/2018jc014781, 2019.
- 649 Mohr, W., Großkopf, T., Wallace, D. W., and LaRoche, J.: Methodological underestimation
650 of oceanic nitrogen fixation rates, PLoS One, 5, e12583,
651 10.1371/journal.pone.0012583.g001, 2010.
- 652 Moisander, P. H., Beinart, R. A., Voss, M., and Zehr, J. P.: Diversity and abundance of
653 diazotrophic microorganisms in the South China Sea during intermonsoon, Isme J, 2,
654 954-967, 10.1038/ismej.2008.51, 2008.
- 655 Moisander, P. H., Zhang, R., Boyle, E. A., Hewson, I., Montoya, J. P., and Zehr, J. P.:
656 Analogous nutrient limitations in unicellular diazotrophs and *Prochlorococcus* in the
657 South Pacific Ocean, Isme J, 6, 733-744, 10.1038/ismej.2011.152, 2012.
- 658 Montoya, J. P., Voss, M., Kähler, P., and Capone, D. G.: A simple, high-precision, high-
659 sensitivity tracer assay for N₂ fixation, Appl. Environ. Microbiol., 62, 986-993,
660 10.1128/AEM.62.3.986-993.1996, 1996.
- 661 Needoba, J. A., Foster, R. A., Sakamoto, C., Zehr, J. P., and Johnson, K. S.: Nitrogen
662 fixation by unicellular diazotrophic cyanobacteria in the temperate oligotrophic
663 North Pacific Ocean, Limnol. Oceanogr., 54, 1317-1327, 10.4319/lo.2007.52.4.1317,
664 2007.
- 665 Rubin, M., Berman-Frank, I., and Shaked, Y.: Dust- and mineral-iron utilization by the



- 666 marine dinitrogen-fixer *Trichodesmium*, *Nat Geosci*, 4, 529-534, 10.1038/ngeo1181,
667 2011.
- 668 Saito, M. A., Goepfert, T. J., and Ritt, J. T.: Some thoughts on the concept of colimitation:
669 Three definitions and the importance of bioavailability, *Limnol. Oceanogr.*, 53, 276-
670 290, 10.4319/lo.2008.53.1.0276, 2008.
- 671 Saito, M. A., Bertrand, E. M., Dutkiewicz, S., Bulygin, V. V., Moran, D. M., Monteiro, F.
672 M., Follows, M. J., Valois, F. W., and Waterbury, J. B.: Iron conservation by reduction
673 of metalloenzyme inventories in the marine diazotroph *Crocospaera watsonii*, *Proc.*
674 *Natl. Acad. Sci. U.S.A.*, 108, 2184-2189, 10.1073/pnas.1006943108, 2011.
- 675 Sañudo-Wilhelmy, S. A., Kustka, A. B., Gobler, C. J., Hutchins, D. A., Yang, M., Lwiza,
676 K., Burns, J. A., Capone, D. G., Ravenk, J. A., and Carpenter, E. J.: Phosphorus
677 limitation of nitrogen fixation by *Trichodesmium* in the central Atlantic Ocean, *Nature*,
678 411, 66-69, 10.1038/35075041, 2001.
- 679 Schlosser, C., Klar, J. K., Wake, B. D., Snow, J. T., Honey, D. J., Woodward, E. M. S.,
680 Lohan, M. C., Achterberg, E. P., and Moore, C. M.: Seasonal ITCZ migration
681 dynamically controls the location of the (sub)tropical Atlantic biogeochemical divide,
682 *Proc. Natl. Acad. Sci. U.S.A.*, 111, 1438-1442, 10.1073/pnas.1318670111, 2014.
- 683 Shiozaki, T., Kodama, T., and Furuya, K.: Large-scale impact of the island mass effect
684 through nitrogen fixation in the western South Pacific Ocean, *Geophys. Res. Lett.*,
685 41, 2907-2913, 10.1002/2014GL059835 2014a.



- 686 Shiozaki, T., Nagata, T., Ijichi, M., and Furuya, K.: Nitrogen fixation and the diazotroph
687 community in the temperate coastal region of the northwestern North Pacific,
688 *Biogeosciences*, 12, 4751-4764, 10.5194/bg-12-4751-2015, 2015a.
- 689 Shiozaki, T., Chen, Y. L. L., Lin, Y. H., Taniuchi, Y., Sheu, D. S., Furuya, K., and Chen, H.
690 Y.: Seasonal variations of unicellular diazotroph groups A and B, and *Trichodesmium*
691 in the northern South China Sea and neighboring upstream Kuroshio Current, *Cont.*
692 *Shelf Res.*, 80, 20-31, 10.1016/j.csr.2014.02.015, 2014b.
- 693 Shiozaki, T., Furuya, K., Kodama, T., Kitajima, S., Takeda, S., Takemura, T., and Kanda,
694 J.: New estimation of N₂ fixation in the western and central Pacific Ocean and its
695 marginal seas, *Global Biogeochem. Cycles*, 24, GB1015, 10.1029/2009gb003620,
696 2010.
- 697 Shiozaki, T., Takeda, S., Itoh, S., Kodama, T., Liu, X., Hashihama, F., and Furuya, K.: Why
698 is *Trichodesmium* abundant in the Kuroshio?, *Biogeosciences*, 12, 6931-6943,
699 10.5194/bg-12-6931-2015, 2015b.
- 700 Shiozaki, T., Bombar, D., Riemann, L., Hashihama, F., Takeda, S., Yamaguchi, T., Ehama,
701 M., Hamasaki, K., and Furuya, K.: Basin scale variability of active diazotrophs and
702 nitrogen fixation in the North Pacific, from the tropics to the subarctic Bering Sea,
703 *Global Biogeochem. Cycles*, 31, 996-1009 10.1002/2017gb005681, 2017.
- 704 Sohm, J. A., Webb, E. A., and Capone, D. G.: Emerging patterns of marine nitrogen fixation,
705 *Nature reviews. Microbiology*, 9, 499-508, 10.1038/nrmicro2594, 2011.



- 706 Sperfeld, E., Raubenheimer, D., and Wacker, A.: Bridging factorial and gradient concepts
707 of resource co-limitation: Towards a general framework applied to consumers, *Ecol.*
708 *Letts.*, 19, 201-215, 10.1111/ele.12554, 2016.
- 709 Stenegren, M., Caputo, A., Berg, C., Bonnet, S., and Foster, R. A.: Distribution and drivers
710 of symbiotic and free-living diazotrophic cyanobacteria in the western tropical South
711 Pacific, *Biogeosciences*, 15, 1559-1578, 10.5194/bg-15-1559-2018, 2018.
- 712 Tanita, I., Shiozaki, T., Kodama, T., Hashihama, F., Sato, M., Takahashi, K., and Furuya,
713 K.: Regionally variable responses of nitrogen fixation to iron and phosphorus
714 enrichment in the Pacific Ocean, *Journal of Geophysical Research: Biogeosciences*,
715 126, e2021JG006542, 10.1029/2021jg006542, 2021.
- 716 Thompson, A. W., Carter, B. J., Turk-Kubo, K. A., Malfatti, F., Azam, F., and Zehr, J. P.:
717 Genetic diversity of the unicellular nitrogen-fixing cyanobacteria UCYN-A and its
718 prymnesiophyte host, *Environ. Microbiol.*, 16, 3238-3249, 10.1111/1462-
719 2920.12490, 2014.
- 720 Turk-Kubo, K. A., Achilles, K. M., Serros, T. R., Ochiai, M., Montoya, J. P., and Zehr, J.
721 P.: Nitrogenase (*nifH*) gene expression in diazotrophic cyanobacteria in the Tropical
722 North Atlantic in response to nutrient amendments, *Front Microbiol.*, 3, 386,
723 10.3389/fmicb.2012.00386, 2012.
- 724 Wang, W. L., Moore, J. K., Martiny, A. C., and Primeau, F. W.: Convergent estimates of
725 marine nitrogen fixation, *Nature*, 566, 205-211, 10.1038/s41586-019-0911-2, 2019.



- 726 Ward, B. A., Dutkiewicz, S., Moore, C. M., and Follows, M. J.: Iron, phosphorus, and
727 nitrogen supply ratios define the biogeography of nitrogen fixation, *Limnol.*
728 *Oceanogr.*, 58, 2059-2075, 10.4319/lo.2013.58.6.2059, 2013.
- 729 Watkins-Brandt, K. S., Letelier, R. M., Spitz, Y. H., Church, M. J., Böttjer, D., and White,
730 A. E.: Addition of inorganic or organic phosphorus enhances nitrogen and carbon
731 fixation in the oligotrophic North Pacific, *Mar. Ecol. Prog. Ser.*, 432, 17-29,
732 10.3354/meps09147, 2011.
- 733 Wen, Z., Browning, T. J., Cai, Y., Dai, R., Zhang, R., Du, C., Jiang, R., Lin, W., Liu, X.,
734 Cao, Z., Hong, H., Dai, M., and Shi, D.: Nutrient regulation of biological nitrogen
735 fixation across the tropical western North Pacific, *Science Advances*, 8, eabl7564,
736 10.1126/sciadv.abl7564, 2022.
- 737 Wu, C., Fu, F. X., Sun, J., Thangaraj, S., and Pujari, L.: Nitrogen fixation by *Trichodesmium*
738 and unicellular diazotrophs in the northern South China Sea and the Kuroshio in
739 summer, *Sci Rep-Uk*, 8, 2415, 10.1038/s41598-018-20743-0, 2018.
- 740 Wu, J., Chung, S. W., Wen, L. S., Liu, K. K., Chen, Y. L. L., Chen, H. Y., and Karl, D. M.:
741 Dissolved inorganic phosphorus, dissolved iron, and *Trichodesmium* in the
742 oligotrophic South China Sea, *Global Biogeochem. Cycles*, 17, 1008,
743 10.1029/2002gb001924, 2003.
- 744 Xu, M. N., Zhang, W., Zhu, Y., Liu, L., Zheng, Z., Wan, X. H. S., Qian, W., Dai, M., Gan,
745 J., Hutchins, D. A., and Kao, S. J.: Enhanced ammonia oxidation caused by lateral



- 746 Kuroshio intrusion in the boundary zone of the northern South China Sea, *Geophys.*
747 *Res. Lett.*, 45, 6585-6593, 10.1029/2018gl077896, 2018.
- 748 Zehr, J. P. and Capone, D. G.: Changing perspectives in marine nitrogen fixation, *Science*,
749 368, eaay9514, 10.1126/science.aay9514, 2020.
- 750 Zhang, R., Zhu, X., Yang, C., Ye, L., Zhang, G., Ren, J. L., Wu, Y., Liu, S. M., Zhang, J.,
751 and Zhou, M.: Distribution of dissolved iron in the Pearl River (Zhujiang) Estuary
752 and the northern continental slope of the South China Sea, *Deep Sea Research Part*
753 *II*, 167, 14-24, 10.1016/j.dsr2.2018.12.006, 2019.